IJCPE
Iraqi Journal of Chemical and Petroleum Engineering

Iraqi Journal of Chemical and Petroleum Engineering
Vol10 No.4 (December 2009) 27-38
ISSN: 1997-4884

University of Baghdad
College of Engineering

Mixed Convection in an Horizontal Rectangular Duct Including interior Circular Core With Time Periodic Boundary Condition

Manal H. AL-Hafidh

Mechanical Engineering Department - College of Engineering - University of Baghdad – Iraq

Abstract

Numerical investigation was done for steady state laminar mixed convection and thermally and hydrodynamic fully developed flow through horizontal rectangular duct including circular core with two cases of time periodic boundary condition, first case on the rectangular wall while keeping core wall constant and other on both the rectangular duct and core walls. The used governing equations are continuity, momentum and energy equations. These equations are normalized and solved using the Vorticity-Stream function and the Body Fitted Coordinates (B.F.C) methods. The finite difference approach with the Line Successive Over-Relaxation (LSOR) method is used to obtain all the computational results. The (B.F.C) method is used to generate the grid of the problem. A computer program (Fortran 90) is built to calculate the Nusselt number (Nu) in steady state. The fluid Prandtl number is 0.7, Rayleigh number (1≤Ra≤106), Reynolds number (1≤Re≤2000). For the range of parameters considered, results show that the time periodic boundary condition enhance heat transfer. It is also indicated in the results that heat transfer from the surface of the circle exceeds that of the rectangle duct. Comparisons with other researches show good agreement.

Keywords: mixed convection, radiation, rectangular duct, circular core, laminar flow, time periodic boundary condition

Introduction

A fully developed mixed convection laminar flow phenomenon occurs in a wide range of engineering applications such as heat exchangers, solar collector, electronic equipment and similar devices. For this purpose various investigations have been performed in the literature under different boundary and operating conditions in order to maximize the heat transfer under optimum channel geometries. Many established models in the literatures explore the distributions of velocity and temperature as well as the heat transfer coefficients between the walls of the ducts and the flow. Although, different shapes of ducts are commonly used in engineering problems, most of the attention of researches has been given to the flow inside a pipe or between two plates or rectangular ducts[Yang and Ebadian, 1991].

[Makinde and Gbolagade, 2005] investigated the second law analysis of a laminar flow of a viscous incompressible fluid through an inclined channel with isothermal walls. Analytical solutions for the fluid velocity and temperature were constructed and the expressions for the entropy generation rate and irreversibility ratio were obtained which show that the heat transfer irreversibility dominates along the channel centerline. A perturbation analysis of combined free and forced laminar convection in a tilted elliptic cylinder was carried out by [Bello-Ochende and Adegun, 1993].
[Nazrul et. al., 2001] performed a numerical and experimental investigation of steady laminar mixed convection heat transfer in horizontal concentric annuli. The thermal boundary condition chosen is that of uniform heat flux at the inner wall and an adiabatic outer wall. it is observed that the Nusselt numbers in the entrance

region are 80-150% greater than the corresponding pure forced convection values.

[Raed, 2007] investigate the steady state laminar mixed convection and radiation through inclined rectangular duct with a varied position circular tube numerically for a hydrodynimacally fully developed flow. A thermal boundary condition of a constant wall temperature is considered. The whole operation of heat transfer inside the channel and the effect of duct inclination angle, radiation and heat generation are studied. The results show generally, Nu will be increased with increasing Ra, radiation, inclination angle and heat generation but it is decreased with geometry ratio and Re increase.

Numerical investigations of unsteady natural convection heat transfer through a fluid saturated porous media in inclined pipe enclosure are studied by [Mohammad, 2008]. The boundary conditions used are insulated upper and lower ends and two cases for the wall; constant wall temperature and sinusoidal varying temperature. The results show that the heat transfer increases with increasing of Rayleigh number, angle of inclination and time. For the time periodic boundary condition case, the temperature increases with amplitude and change its behavior with the change of period and hot regions formed with the increase of amplitude.

Experimental Work

The steady state laminar mixed convection through horizontal rectangular duct including circular core with two cases of time periodic boundary condition is investigated numerically for a thermally and hydrodynamic fully developed flow. The schematic drawing of the geometry and the Cartesian coordinate system employed in solving the problem is shown in Fig.(1).

The flow is accurate between the circular core and the rectangular duct (Annulus). This annulus is symmetrical about Y-axis ($\partial/\partial x = 0$). The width and height of the channel are W and H respectively. The diameter and radius of core are D and R respectively and the hydraulic diameter is dH:

$$d_H = \frac{4A}{P^*} = \frac{2(HL - \pi R^2)}{(H + L + \pi R)} \quad (1)$$

The fluid properties are assumed to be constant except for density variation with temperature resulting in the secondary flows generated by the buoyancy forces. The axial (z) direction is shown in Fig. (1) and is the predominant direction for the fluid flow. The flow is laminar, and viscous dissipation effects are neglected. Axial conduction and radiation are assumed negligible following [Yang and Ebadian, 1991].

Governing Equations:

The governing equations are **[Adegun and Bello, 2004]**:

Continuity Equation

$$\frac{\partial u}{\partial x} + \frac{\partial v}{\partial y} = 0 \quad (2)$$

Momentum Transport Equation

The momentum transport equations in the x, y and z directions are respectively:

$$u\frac{\partial u}{\partial x} + v\frac{\partial u}{\partial y} = -\frac{1}{\rho}\frac{\partial p}{\partial x} + \nu\,\Delta^2 u \quad (3)$$

$$u\frac{\partial v}{\partial x} + v\frac{\partial v}{\partial y} = -\frac{1}{\rho}\frac{\partial p}{\partial y} + \nu\,\Delta^2 v - \beta\, g(T_w - T)\cos\lambda \quad (4)$$

$$u\frac{\partial w}{\partial x} + v\frac{\partial w}{\partial y} = -\frac{1}{\rho}\frac{\partial p}{\partial z} + \nu\,\Delta^2 w - \beta\, g(T_w - T)\sin\lambda \quad (5)$$

Energy Transport Equation

In the absence of energy sources and viscous energy dissipation, the energy equation for steady flow, with radiation incorporated is:

$$u\frac{\partial T}{\partial x} + v\frac{\partial T}{\partial y} + w\frac{\partial T}{\partial z} = \alpha\left(\frac{\partial^2 T}{\partial x^2} + \frac{\partial^2 T}{\partial y^2}\right) \quad (6)$$

Normalization Parameters

The variables in the governing equations and boundary conditions are transformed to dimensionless formula by employing the following transformation parameters:

$$X = \frac{x}{d_H}, \quad Y = \frac{y}{d_H}, \quad Z = \frac{z}{d_H}$$

$$\tau' = \frac{t}{\rho\, cp\, D^2/k}, \quad \eta' = \frac{per}{D^2/(k/\rho\, cp)}, \quad a = \frac{A_1}{\Delta T}$$

$$U = \frac{u d_H}{\nu}, \quad V = \frac{v d_H}{\nu}, \quad W = \frac{w d_H}{\nu}$$

$$\theta = \frac{T}{T_w}, \quad \frac{\partial p}{\partial z} = -\frac{4\rho\nu^2}{d_H^3}\mathrm{Re}, \quad \frac{\partial T}{\partial z} = \frac{T_w}{\mathrm{Pr}\, d_H}, \quad \mathrm{Pr} = \frac{\nu}{\alpha}$$

$$U = \frac{\partial \psi}{\partial Y} \quad , \quad V = -\frac{\partial \psi}{\partial X}$$

After eliminating the pressure terms in the two momentum equations in X and Y directions by cross differentiation and using vorticity-stream function method, the governing equations in the dimensionless form become:

$$\frac{\partial \psi}{\partial Y}\frac{\partial \omega}{\partial x} - \frac{\partial \psi}{\partial X}\frac{\partial \omega}{\partial Y} = \left(\frac{\partial^2 \omega}{\partial X^2} + \frac{\partial^2 \omega}{\partial Y^2}\right) - \frac{R_a \cos\lambda}{\Pr}\frac{\partial \theta}{\partial X} \qquad (7)$$

Stream Function Equation

$$-\omega = \frac{\partial^2 \psi}{\partial X^2} + \frac{\partial^2 \psi}{\partial Y^2} \qquad (8)$$

Axial Momentum Equation

$$\frac{\partial \psi}{\partial Y}\frac{\partial W}{\partial X} - \frac{\partial \psi}{\partial X}\frac{\partial W}{\partial Y} = \left(\frac{\partial^2 W}{\partial X^2} + \frac{\partial^2 W}{\partial Y^2}\right) + 4\mathrm{Re} - \frac{Ra \sin\lambda}{\Pr}(1-\theta) \qquad (9)$$

$$\frac{\partial \psi}{\partial Y}\frac{\partial \theta}{\partial X} - \frac{\partial \psi}{\partial X}\frac{\partial \theta}{\partial Y} = \frac{1}{\Pr}\left(\frac{\partial^2 \theta}{\partial X^2} + \frac{\partial^2 \theta}{\partial Y^2}\right) - \frac{W}{\Pr} \qquad (10)$$

The boundary conditions applicable to these equations are [Adegun and Bello, 2004]:

(1) At the inlet of the duct (Z= 0):

$$U = V = W = \psi = 0 \qquad \text{(No slip condition)}$$

$$\theta = 0.5 \quad , \quad W = \frac{\mathrm{Re}}{v d_H}$$

(2) At the walls:

$$U = V = W = \psi = 0$$

Case 1 $\theta = 1 + a \sin(2\pi\tau/\acute{\eta})$ rectangular duct wall

$\theta = 1$ circular core wall

Case 2 $\theta = 1 + a \sin(2\pi\tau/\acute{\eta})$ rectangular duct wall

$\theta = 1 + a \sin(2\pi\tau/\acute{\eta})$ circular core wall

$$\frac{\partial \theta}{\partial X} = \frac{\partial \psi}{\partial X} = \frac{\partial \omega}{\partial X} = \frac{\partial W}{\partial X} = 0 \qquad \text{(at symmetry line)}$$

Numerical Methods

Numerical Grid Generation:

The elliptic transformation technique which was originally proposed by **[Fletcher, 1988]** is applied to generate the curvilinear grid for dealing with the irregular cross sections. The transformation functions $\xi = \xi(X,Y)$ and $\eta = \eta(X,Y)$ are obtained to accommodate the irregular shape by solving the following partial differential equations:

$$\frac{\partial^2 \xi}{\partial X^2} + \frac{\partial^2 \xi}{\partial Y^2} = G(\xi,\eta) \qquad (11)$$

$$\frac{\partial^2 \eta}{\partial x^2} + \frac{\partial^2 \eta}{\partial Y^2} = S(\xi,\eta) \qquad (12)$$

Where G and S are two functions and are defined to artificially adjust the density of the grid locally. Using the curvilinear grid obtained, the governing eq. (7) to (10) and the boundary conditions are then discretized and solved in the computation domain (ξ,η). In this work, an (81 X 61) grid in the transformed domain $(\xi \mathrm{X} \eta)$ is adopted. **Fig. (2)** shows typical grid generated for the channel cross section. The grid systems have been properly adjusted to be orthogonal locally at the boundaries. The grid generation technique used is standard and well accepted. Therefore, further description about this technique would not give here.

By using this method, the following general equation can be used to generate all the governing –equations (7-10) in computational coordinate's formula:

$$J\Gamma\left(\psi_\eta \phi_\xi - \psi_\xi \phi_\eta\right) = \left(\tau\phi_\xi + \varpi\phi_\eta + \alpha_1\phi_{\xi\xi} - 2\beta_1\phi_{\xi\eta} + \gamma\phi_{\eta\eta}\right) + suJ^2 \qquad (13)$$

Where Φ represent the general variable which may be ω, W or θ and su is the source term.

Finite Difference Formulation:

The three-point central difference formula is applied to all the derivatives. Each of the governing equations can be rewritten in a general form as:

$$ap_{(i,j)}\phi_{(i,j)} = ae_{(i,j)}\phi_{(i+1,j)} + aw_{(i,j)}\phi_{(i-1,j)} + an_{(i,j)}\phi_{(i,j+1)} as_{(i,j)}\phi_{(i,j-1)} + SU_{(I,J)}J_{(I,J)} \qquad (14)$$

Where:

$$ap(i,j) = 2\left(\alpha_1(i,j) + \gamma(i,j)\right)$$

$$ae(i,j) = \alpha_1(i,j) - B$$

$$aw(i,j) = \alpha_1(i,j) + B$$

$$an(i,j) = \gamma(i,j) - C$$

$$as(i,j) = \gamma(i,j) + C$$

$$B = \left(J_{(i,j)}\Gamma \frac{\psi_{(i+1,j)} - \psi_{(i-1,j)}}{2} - \tau_{(i,j)} \right) \Big/ 2$$

$$C = \left(-J_{(i,j)}\Gamma \frac{\psi_{(i,j+1)} - \psi_{(i,j-1)}}{2} - \varpi_{(i,j)} \right) \Big/ 2$$

$$SU_{(I,J)} = -\frac{\beta_{1(i,j)}}{2J_{(i,j)}} \left(\phi_{(i+1,j+1)} - \phi_{(i+1,j-1)} - \phi_{(i-1,j+1)} + \phi_{(i-1,j-1)} \right) + su_{(i,j)} J_{(i,j)}$$

In the equations above i and j indicate to the points of the grid in the generalized coordinates ξ and η respectively.

As pointed out in [Anderson, 1984] the Relaxation method can be employed for the numerical solution of the eq. (8). For this study, the LSOR method [Fletcher, 1988 and Anderson, 1984] is used to solve equations (7, 9 and 10). The convergence criterion for the inner iteration ($Error_{in}$) of ψ is 10^{-4} and for the outer iteration ($Error_{out}$) of θ_b is 10^{-10}, where:

$$Error_{in} = 2\left(\alpha_{1(i,j)} + \gamma_{(i,j)}\right)\Delta\psi_{(i,j)} \qquad (15)$$

$$\Delta\psi_{(i,j)} = \frac{\psi^{it+1}_{(i,j)} - \psi^{it}_{(i,j)}}{RP} \qquad (16)$$

Where RP is the over – Relaxation factor and equal 1.1 and *it* represents the number of iterations. The outer iteration is checked only for θ_b as follow:

$$Error_{out} = \frac{\theta^{it+1}_b - \theta^{it}_b}{\theta^{it}_b} \leq 10^{-10} \qquad (17)$$

Evaluation of Heat Transfer:

The peripheral heat transfer is defined through the conduction referenced Nusselt number as:

Local Nusselt number

The peripheral local Nusselt number on the walls of the channel is computed from:

$$Nu_L = \frac{-\frac{\partial\theta}{\partial n}\Big|_w}{(1-\theta_b)} \qquad (18)$$

Where *n* represent the dimensionless normal outward direction.

The mean Nusselt number on the wall of the rectangular duct and circular core is obtained by using Simpson's rule:

$$Nu_{c,r} = \frac{1}{s}\int_s Nu_L\, ds \qquad (19)$$

Where s is represents the length of the wetted perimeter in the rectangular duct and circular core.

The mean Nusselt number (Nu) is a measure of the average heat transfer over the internal surface of the rectangular duct and the outer surface of the circular configuration. It is computed from the following equation:

$$Nu = C_c\, Nu_c + C_r Nu_r \qquad (20)$$

Where, C_C Nu_C is a measure of average heat transfer from the outer surface of the circular core while C_r Nu_r corresponds to heat transfer from the internal surface of the rectangular duct. Cc and Cr are the perimetric ratios for the heat transfer and are defined as [Adegun and Bello, 2004]:

$$C_c = \frac{\pi R}{H + L + \pi R}$$

$$C_r = \frac{H + L}{H + L + \pi R}$$

Results and Discussion

Isotherms and Streamlines

Figures (2-3) and Figures (4-5) illustrate the isotherms and streamlines for different values of dimensionless period ή and constant dimensionless time τ for $Ra=10^3$ and $Ra=10^4$ respectively. These figures show that the decrease in ή and increase in Ra will increase the intensity and the value of stream function and the temperature of the fluid and enhance the heat transfer because the heat transferred to the cylinder is very high at the beginning of heating and this is clear in contour plots which indicates a strong buoyancy effect from the first instant of process. The effect of amplitude on the convective fluid is shown in Figures (6-7) and it is clear that the increase in amplitude because the isotherm lines to lost its uniformity and an increase in heat transfer is shown at the surface of the circular core. Figures (8-9) illustrate the isotherms and streamlines for $Ra=10^6$ and Re =1000 and 2000 for case1 and case2 respectively. It is clear from figures that the increase of Re cause a strong convective flow and a strong buoyancy effect and an increase in temperature will be indicated.

Effect of Ra

Figures (10-11) and Figures (12-13) for $Ra=10^5$ and $Ra=10^6$ respectively show the effect of increasing Ra and Re on Nu for case1 and case2. Nu decrease with increasing of Re until Re=1000 then increase this indicate that the velocity opposite its direction in early times, but the increasing of Ra means an increase in temperature and velocity which in turn increase Nu. Figures (14-15) show that heat transfer increase for case1 where the periodic boundary condition applied for the rectangular duct only and enhanced more for case2 where the periodic boundary condition applied for both the rectangular duct and the cylindrical core walls. From the comparison of the present work with other research Figures (16-17) illustrate that an increase in heat transfer is clear for the present work compared with [Raed, 2007] who take constant wall temperatures boundary conditions for both the rectangular duct and the cylindrical core..

Conclusions

1. For the first time, *Trichoderma harizanum* and *Pleurotus ostreatus* were proven through this study to be considered hydrocarbon degrading microorganisms.
2. *Trichoderma harizanum* which is known as biological control and fertilizer called "Al-Tahadi" is proved to have an important role in this biotreatment according to the activity of producing extra cellular enzymes.
3. The suitability of using different cheap and available agricultural wastes substrate in the cultivation of *Pleurotus ostreatus* will lead to the use of this fungus in wide range of biological treatment or control.
4. The used biotreatment can be considered as an effective treatment option since most of used materials at incubation and growth of microorganisms were available and cheap.
5. Specific local conditions can affect the biological activity. For example, certain levels of temperature degrees can limit all microbial activity and reduce the rate of hydrocarbon biodegradation. The study showed that the optimum humidity and temperature were 15 to 35 % and 20 to 40° C respectively.
6. The best hydrocarbon degradation occurred by using the two microorganisms together with 5% by weight concentration ratio and with nutrient addition (5% by weight nutrient concentration and C/N/P=100/50/10 as nutrients components ratio). Here the best average of total petroleum hydrocarbon degradation was 205 ppm/day.

References

1. McMillen, S.J., R.Smart, R. Bernier, and R.E. Hoffman: "Biotreating E & P Wastes: Lessons Learned from 1992-2003," SPE 86794, presented at the Seventh International Conference on Health, Safety Environment in Oil and Gas Exploration and Production, Calgary, Alberta, Canada, March 29-31 (2004).
2. McMillen, S.J., R.Smart, R. Bernier, and R.E. Hoffman: "Biotreating E & P Wastes: Lessons Learned from 1992-2003," SPE 86794, presented at the Seventh International Conference on Health, Safety Environment in Oil and Gas Exploration and Production, Calgary, Alberta, Canada, March 29-31 (2004).
3. ZoBell, C. E.: "Assimilation of hydrocarbons by microorganisms", Adv. Enzymol, no. 10, pp. 443-486, (1950).
4. Beerstecher, E.: "Petroleum Microbiology," Elsevier Publishing Company, Amsterdam, pp. 375, (1954).
5. Davis, J. B.: "Petroleum Microbiology," Elsevier Publishing Company, Amsterdam, London, NewYork, (1967).
6. Environmental Protection Agency (EPA): "Land Fariming In: How to Evaluate Alternative Cleanup Technologies for Underground Storage Tank Sites: A Guide for Corrective Action Plan Reviews," EPA, 510-B-94-003 and EPA 510-B-95-007. (1994).
7. Hassan, A. A. K.: "Production of Fibrinolytic Proteas from Pleurotus ostreatus by Solid State Fermentation," Ph. D. Thesis University of Baghdad, (2005).
8. Atlas, R. M., and Bartha, R.: "Hydrocarbon Biodegradation and Oil Spill Bioremediation," Advances in Microbial Ecology, 12, pp. 287-388, (1992).
9. Chaineau, C. H., Morel, J. L., and Oudot, J.: "Biodegradation of Fuel Oil Hydrocarbons in The Rhizophere of Maize, J. Environ. Qual., 29, pp. 569-578, (2000).
10. Zimmerman, P.K., and Robert, J. D.: "Oil – Based Drill Cuttings Treated by Landfarming," Oil and Gas Journal, 81 (1991).
11. Chaineau, C. H., Morel, J. L., and Oudot, J.: "Land Treatment of Oil Based Drill Cutting in an Agricultural Soil," J. Environ. Qual., 25, 858 – 867 (1996).
12. Quimio, T. H. ; Chang, S. T. and Royes, D. J. "Technical guidelines for mushroom growing in the tropics. "FAO. Plant Production and Protection, paper 106 , Rome , Italy (1990).
13. Page, Paul, 2006. Pers Comm.. on 17.8.2006. with Paul Page of BP Exploration, England, United Kingdom.
14. Bossert, I., and Bartha, R.: "The Fate of Petroleum in Soil Ecosystem," p. 435-476. In R.M. Ahasled, Petroleum Microbiology, Macmillan Co. New York. (1984).

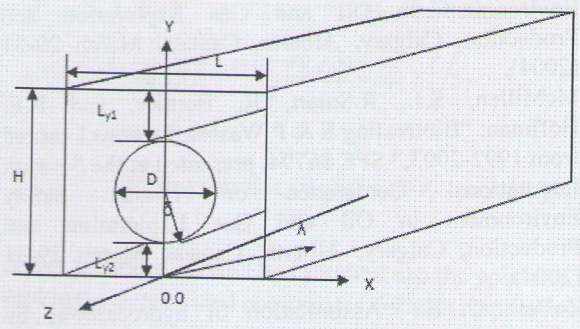

Fig. (1) Schematic of the Problem Geometry

Level	Temp.
15	1.00356
14	1.00308
13	1.00259
12	1.00211
11	1.00162
10	1.00114
9	1.00065
8	1.00017
7	0.999682
6	0.999197
5	0.998712
4	0.998227
3	0.997742
2	0.997257
1	0.996772

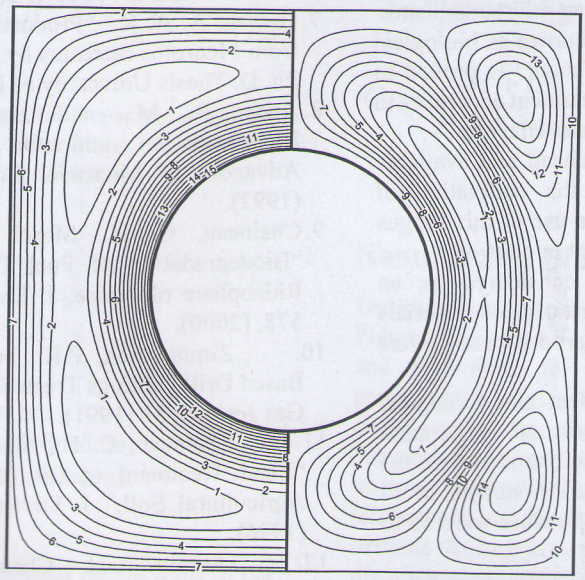

Level	Stream
15	0.000138023
14	0.000111806
13	8.55902E-05
12	5.9374E-05
11	3.31579E-05
10	6.94167E-06
9	-1.92745E-05
8	-4.54907E-05
7	-7.17069E-05
6	-9.79231E-05
5	-0.000124139
4	-0.000150355
3	-0.000176572
2	-0.000202788
1	-0.000229004

Fig. 2 The Isotherms and Streamlines for case1,Ra=10^3
Re=1 and τ^{*}=0.02, $\acute{\eta}$=0.01 and a=0.8

Level	Temp.
15	1.00734
14	1.00659
13	1.00584
12	1.00509
11	1.00434
10	1.00359
9	1.00284
8	1.00209
7	1.00135
6	1.0006
5	0.999846
4	0.999096
3	0.998346
2	0.997597
1	0.996847

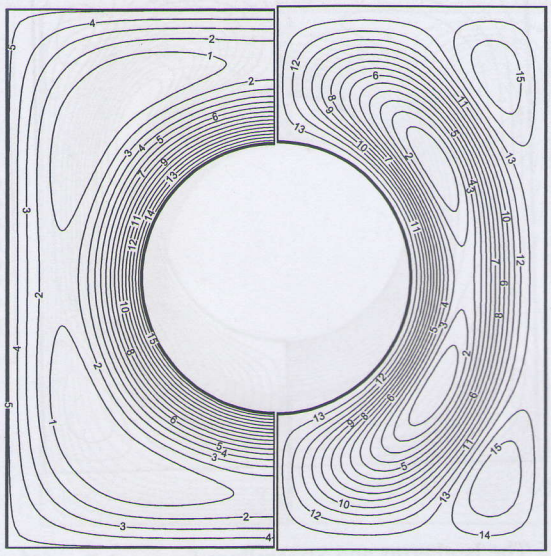

Level	Stream
15	5.72847E-05
14	1.66972E-05
13	-2.38904E-05
12	-6.4478E-05
11	-0.000105066
10	-0.000145653
9	-0.000186241
8	-0.000226828
7	-0.000267416
6	-0.000308003
5	-0.000348591
4	-0.000389179
3	-0.000429766
2	-0.000470354
1	-0.000510941

Fig. 3 The Isotherms and Streamlines for case1,Ra=10^3
Re=1 and τ^{*} =0.02, ή=0.005and a=0.8

Level	Temp.
15	1.00341
14	1.00277
13	1.00214
12	1.0015
11	1.00087
10	1.00023
9	0.999593
8	0.998956
7	0.99832
6	0.997684
5	0.997048
4	0.996412
3	0.995776
2	0.995139
1	0.994503

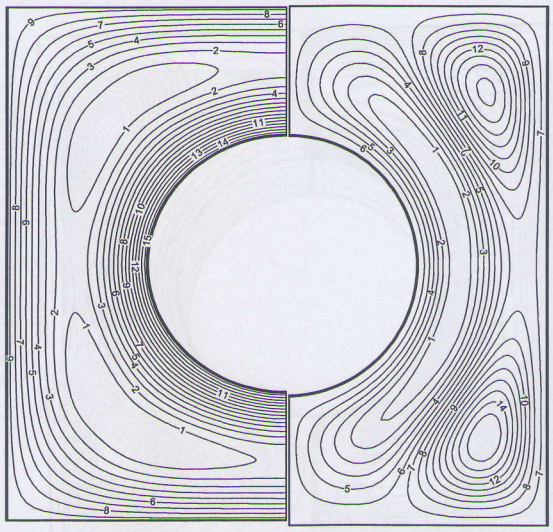

Level	Stream
15	0.00316892
14	0.00279008
13	0.00241125
12	0.00203242
11	0.00165359
10	0.00127475
9	0.00089592
8	0.000517087
7	0.000138254
6	-0.000240578
5	-0.000619411
4	-0.000998244
3	-0.00137708
2	-0.00175591
1	-0.00213474

Fig.4 The Isotherms and Streamlines for case1,Ra=10^4
Re=1 and τ^{*}=0.02, ή=0.01 and a=0.8

Level	Temp.
15	1.00735
14	1.0066
13	1.00586
12	1.00512
11	1.00437
10	1.00363
9	1.00289
8	1.00214
7	1.0014
6	1.00066
5	0.999913
4	0.99917
3	0.998426
2	0.997682
1	0.996939

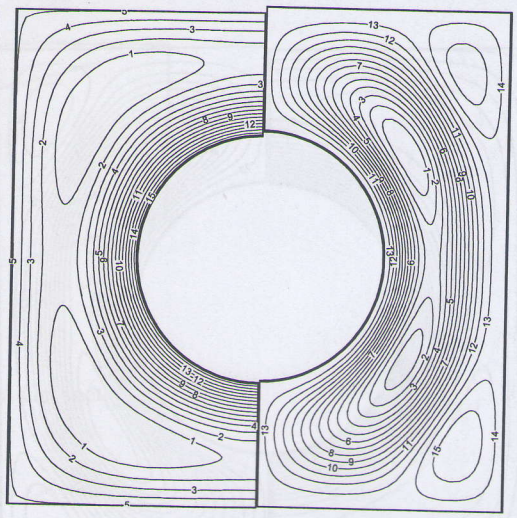

Level	Stream
15	0.000527473
14	0.000118822
13	-0.000289828
12	-0.000698478
11	-0.00110713
10	-0.00151578
9	-0.00192443
8	-0.00233308
7	-0.00274173
6	-0.00315038
5	-0.00355903
4	-0.00396768
3	-0.00437633
2	-0.00478498
1	-0.00519363

Fig.5 The Isotherms and Streamlines for case1,Ra=10^4
Re=1 and $\tau^{'}$=0.02, $\acute{\eta}$=0.05 and a=0.8

Level	Temp.
15	1.00146
14	1.00089
13	1.00032
12	0.999758
11	0.999192
10	0.998626
9	0.99806
8	0.997494
7	0.996928
6	0.996362
5	0.995795
4	0.995229
3	0.994663
2	0.994097
1	0.993531

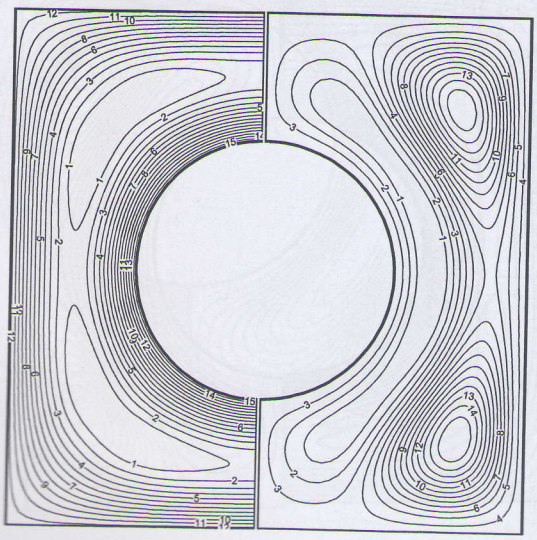

Level	Stream
15	0.000454116
14	0.000414138
13	0.000374161
12	0.000334183
11	0.000294205
10	0.000254227
9	0.00021425
8	0.000174272
7	0.000134294
6	9.43165E-05
5	5.43387E-05
4	1.4361E-05
3	-2.56168E-05
2	-6.55945E-05
1	-0.000105572

Fig.6 The Isotherms and Streamlines for case1,Ra=10^3
Re=1 and $\tau^{'}$=0.02, $\acute{\eta}$=0.01 and a=0.2

Level	Temp.
15	1.00165
14	1.00128
13	1.00091
12	1.00054
11	1.00017
10	0.9998
9	0.99943
8	0.999059
7	0.998689
6	0.998318
5	0.997948
4	0.997578
3	0.997207
2	0.996837
1	0.996466

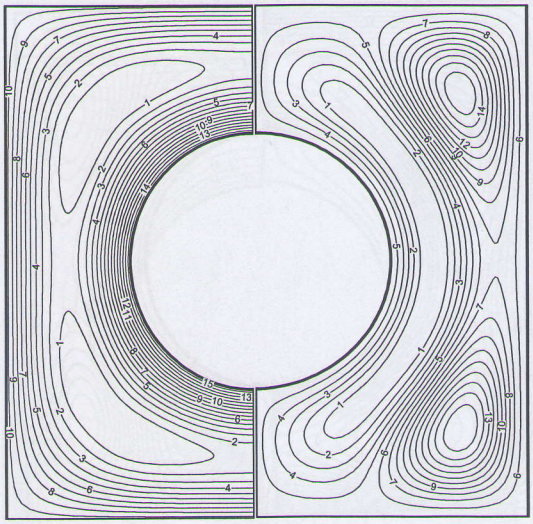

Level	Stream
15	0.000215497
14	0.00019277
13	0.000170043
12	0.000147317
11	0.00012459
10	0.000101863
9	7.91368E-05
8	5.64101E-05
7	3.36834E-05
6	1.09567E-05
5	-1.17699E-05
4	-3.44966E-05
3	-5.72233E-05
2	-7.99499E-05
1	-0.000102677

Fig.7 The Isotherms and Streamlines for case1,Ra=10^3
Re=1 and $\tau^{'}$ =0.02, ή=0.01 and a=0.4

Level	Temp.
15	0.979821
14	0.955597
13	0.931372
12	0.907147
11	0.882923
10	0.858698
9	0.834474
8	0.810249
7	0.786024
6	0.7618
5	0.737575
4	0.71335
3	0.689126
2	0.664901
1	0.640677

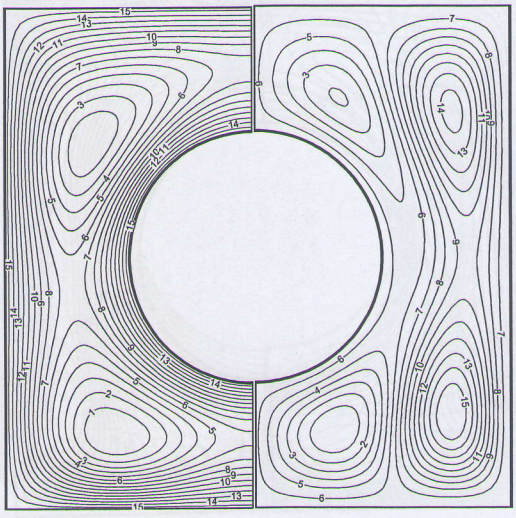

Level	Stream
15	1.74245
14	1.54088
13	1.33931
12	1.13774
11	0.936167
10	0.734596
9	0.533024
8	0.331453
7	0.129882
6	-0.0716895
5	-0.273261
4	-0.474832
3	-0.676403
2	-0.877974
1	-1.07955

Fig.8 The Isotherms and Streamlines for case1,Ra=10^5
Re=1000 and $\tau^{'}$ =0.02, ή=0.01and a=0.8

Level	Temp.
15	0.979838
14	0.95563
13	0.931422
12	0.907215
11	0.883007
10	0.858799
9	0.834591
8	0.810383
7	0.786176
6	0.761968
5	0.73776
4	0.713552
3	0.689344
2	0.665136
1	0.640929

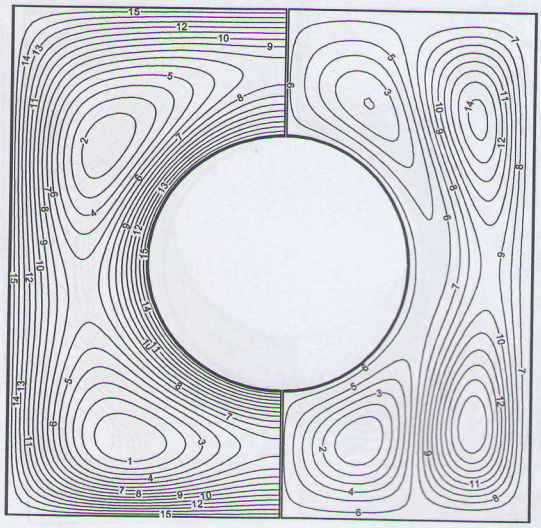

Level	Stream
15	1.78325
14	1.58019
13	1.37713
12	1.17406
11	0.971002
10	0.767939
9	0.564876
8	0.361813
7	0.158749
6	-0.0443136
5	-0.247377
4	-0.45044
3	-0.653503
2	-0.856566
1	-1.05963

Fig.9 The Isotherms and Streamlines for case2,Ra=10^5
Re=1000 and τ' =0.02, ή=0.01and a=0.8

Level	Temp.
15	0.983505
14	0.962964
13	0.942422
12	0.921881
11	0.90134
10	0.880799
9	0.860258
8	0.839716
7	0.819175
6	0.798634
5	0.778093
4	0.757552
3	0.737011
2	0.716469
1	0.695928

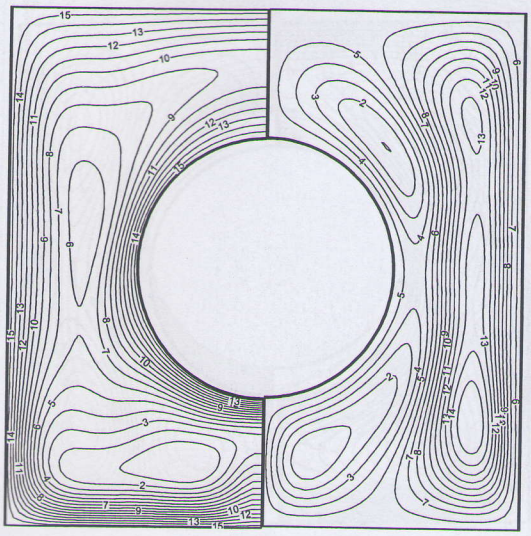

Level	Stream
15	6.97957
14	6.23703
13	5.49449
12	4.75194
11	4.0094
10	3.26685
9	2.52431
8	1.78177
7	1.03922
6	0.296678
5	-0.445866
4	-1.18841
3	-1.93095
2	-2.6735
1	-3.41604

Fig.10 The Isotherms and Streamlines for case1,Ra=10^6
Re=1000 and τ' =0.02, ή=0.01and a=0.8

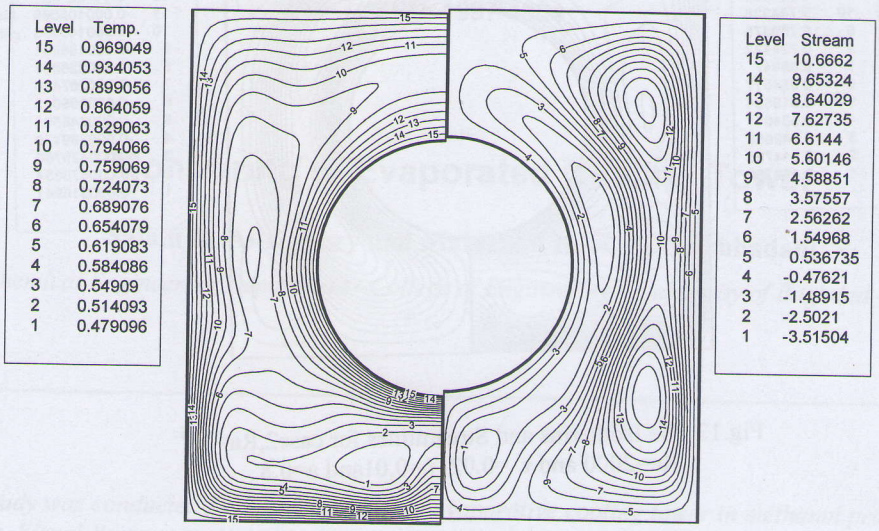

Fig.11 The Isotherms and Streamlines for case1,Ra=10^6
Re=2000 and $\tau^{'}$ =0.02, ή=0.01and a=0.8

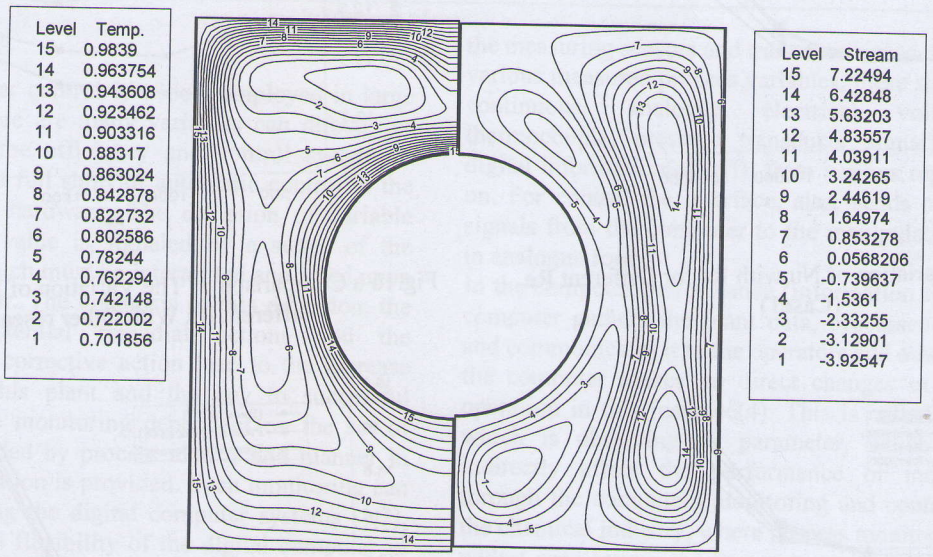

Fig.12 The Isotherms and Streamlines for case1,Ra=10^6
Re=2000 and $\tau^{'}$ =0.02, ή=0.01and a=0.8

Level	Temp.
15	0.969093
14	0.93414
13	0.899187
12	0.864234
11	0.829281
10	0.794328
9	0.759375
8	0.724422
7	0.68947
6	0.654517
5	0.619564
4	0.584611
3	0.549658
2	0.514705
1	0.479752

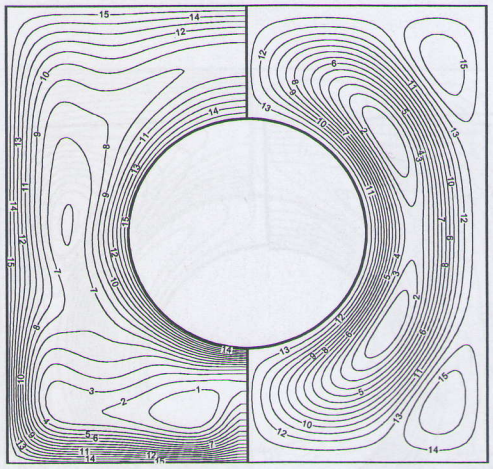

Level	Stream
15	5.72847E-05
14	1.66972E-05
13	-2.38904E-05
12	-6.4478E-05
11	-0.000105066
10	-0.000145653
9	-0.000186241
8	-0.000226828
7	-0.000267416
6	-0.000308003
5	-0.000348591
4	-0.000389179
3	-0.000429766
2	-0.000470354
1	-0.000510941

Fig.13 The Isotherms and Streamlines for case2,Ra=10^6
Re=2000 and τ^{*} =0.02, ή=0.01and a=0.8

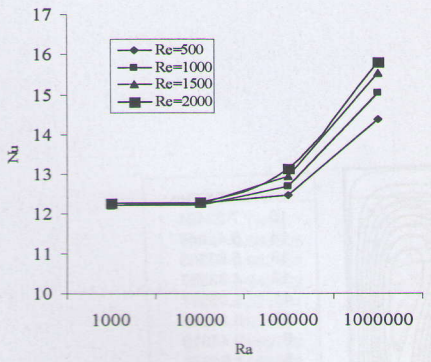

Fig. 14 the Variation of Nu with Ra for Different Re (Case1)

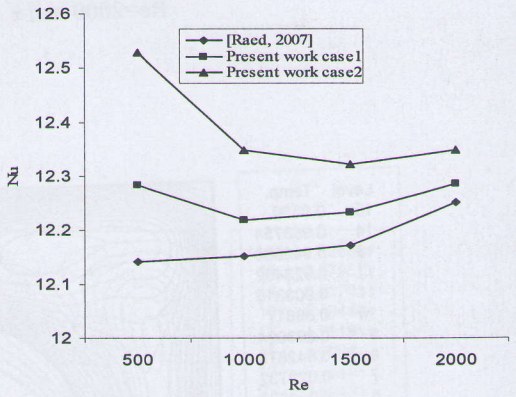

Fig.16 a Comparison of The Variation of Nu with Re for Different Ra With Other research

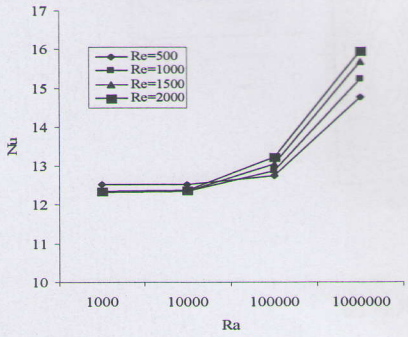

Fig. 15 the Variation of Nu with Ra for Different Re (Case2)

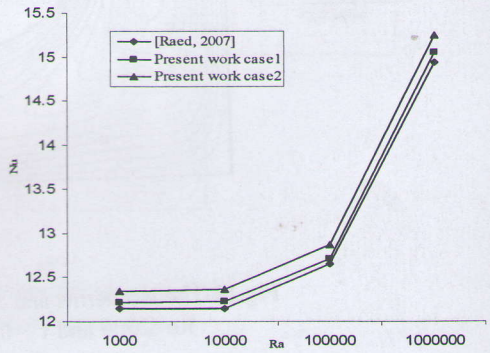

Fig.17 a Comparison of The Variation of Nu with Ra for Different Re with Other research